

# Propagation Characteristics of Single-Mode Optical Fibers With Arbitrary Complex Index Profiles

Xin Qian, *Student Member, IEEE*, and Anthony C. Boucouvalas, *Fellow, IEEE*

**Abstract**—A rapidly converging numerical technique for the evaluation mode characteristics of circularly symmetric optical fibers with an arbitrary complex refractive index profile is presented. This method is based on transmission-line principles. From Maxwell's equations, we derive a transmission-line equivalent circuit for the optical fiber refractive index profile and we demonstrate how it can be used to determine the mode effective index (normalized propagation constant) of cylindrical dielectric waveguides. To illustrate the effectiveness of the procedure, we have applied it to circularly symmetric fibers with complex step, parabolic, and segmented optical refractive index profiles. We have used this method to evaluate and manipulate the gain in a typical 980-nm pumped erbium-doped fiber as well as for calculating attenuation of optical fibers when radial loss factors are present.

**Index Terms**—Erbium-doped fiber amplifiers (EDFA), gain, single-mode fiber.

## I. INTRODUCTION

**E**RBIUM-DOPED fiber amplifiers (EDFAs) have now replaced optoelectronic repeaters as the primary design option for extending the range and capacity of the world's fiber-optic telecommunications systems [1]. These amplifiers naturally provide gain at very high bit rates and at many wavelengths in a broad band stretching from 1.53 to 1.58  $\mu\text{m}$ . With the advent of fiber lasers and doped fiber amplifiers, attention has been drawn to the analysis of optical fibers whose refractive index profile can be described in terms of a complex numbers. Complex refractive index profiles result in complex mode propagation constants offering information on the loss or gain properties of optical fibers. Some approximate or numerically cumbersome methods have been reported in the literature [2]–[5] for evaluation of the propagation characteristics of such fibers. The authors of [2] attempt to separate the real and imaginary parts of the complex scalar wave equation to obtain two real scalar wave equations, under the assumption that the imaginary part of the field is much smaller than the real part. Thus, this method is accurate only for profiles in which the imaginary part of the refractive index is very small. Reference [3] has been the standard method of perturbation, in which the restraining assumption is that the loss or gain exhibited by the fiber does not significantly alter the field and is also valid for small imaginary parts of the refractive index. To

overcome this restraint, a numerical procedure (Rayleigh–Ritz) was developed [4], [5], involving expansion of the mode field in terms of appropriate basic functions. This procedure has been extended to complex refractive index profiles by choosing complex expansion coefficients. This converts the problem to a complex matrix eigenvalue equation. Although this procedure does not neglect the imaginary part of the field, the number of basic functions required in the expansion, for sufficient accuracy, can often be as large as 50. Hence, the procedure requires evaluation of the complex eigenvalues of a  $50 \times 50$  matrix with complex elements. This requires a cumbersome algorithm, as well as the use of optimized NAG library routines, and it is relatively slow in obtaining an eigenvalue.

We have shown that transmission-line techniques can be applied in optical fibers with real refractive index profiles and can determine exactly the mode propagation constants [6] and cut-off wavelengths of waveguide modes [7]. In general, from knowledge of the mode electric field, we can even synthesize the exact refractive index profiles numerically using this powerful technique [8].

In this paper, we are presenting a simple direct numerical procedure to evaluate accurately the complex propagation constants in circularly symmetric single-mode fibers with an arbitrary complex refractive index profile. It is based on the transmission-line principles. Section II describes the basic theory our technique is based upon.

## II. TRANSMISSION-LINE REPRESENTATION OF OPTICAL FIBERS

We divide a cylindrical optical waveguide into a large number of concentric homogeneous cylindrical layers of thickness  $\delta r$ , permittivity  $\epsilon$ , permeability  $\mu$ , and conductivity  $\sigma$  in Fig. 1.

The  $E$  and  $H$  components of Maxwell's equations for any such layer can be written as [6]

$$\left. \begin{aligned} \beta r E_\theta - l E_Z &= \omega \mu r H_r \\ l H_Z - \beta r H_\theta &= (\omega \epsilon - j \sigma) r E_r \\ \frac{\partial(\omega \mu r H_r)}{\partial r} &= -j \omega \mu (l H_\theta + \beta r H_Z) \end{aligned} \right\} (1)$$

$$\left. \begin{aligned} \frac{\partial[(\omega \epsilon - j \sigma) r E_r]}{\partial r} &= -(\sigma + j \omega \epsilon)(l E_\theta + \beta r E_Z) \\ \frac{\partial(l H_\theta + \beta r H_Z)}{\partial r} &= -\frac{\gamma^2}{j \omega \mu} \omega \mu r H_r + \beta H_Z - \frac{l}{r} H_\theta \\ \frac{\partial(l E_\theta + \beta r E_Z)}{\partial r} &= -\frac{\gamma^2}{\sigma + j \omega \epsilon} (\omega \epsilon - j \sigma) r E_r + \beta E_Z - \frac{l}{r} E_\theta \end{aligned} \right\} (2)$$

where  $\gamma^2 = \beta^2 + (l/r)^2 - \omega^2 \mu \epsilon + j \omega \mu \sigma$ ,  $\beta$  is the propagation constant,  $l$  is the azimuthal mode number (integer), and  $\omega$  is the mode frequency.

Manuscript received September 17, 2003; revised February 11, 2004.  
The authors are with the M<sup>2</sup>C Research Group, Bournemouth University, Bournemouth BH12 5BB, U.K. (e-mail: qxian@bournemouth.ac.uk).  
Digital Object Identifier 10.1109/JQE.2004.828244

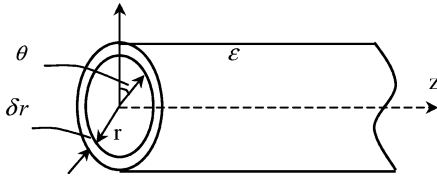


Fig. 1. Homogeneous optical fiber thin cylindrical layer.

We restrict our analysis to the case  $\sigma = 0$ ,  $\mu = \mu_0$ ,  $\epsilon = n^2 \epsilon_0$ , where  $n$  is the refractive index of the layer at distance  $r$  from the axis. We define the following variable voltages and currents:

$$\left. \begin{aligned} V_s &= \frac{V_M}{\sqrt{n}} + V_E \sqrt{n} & (\text{sum}) \\ V_d &= \frac{V_M}{\sqrt{n}} - V_E \sqrt{n} & (\text{difference}) \\ I_s &= I_M \sqrt{n} + \frac{I_E}{\sqrt{n}} & (\text{sum}) \\ I_d &= I_M \sqrt{n} - \frac{I_E}{\sqrt{n}} & (\text{difference}) \end{aligned} \right\} \quad (3)$$

where

$$\begin{aligned} V_M &= \frac{lH_\theta + \beta r H_z}{jF} Z_0 & (\text{magnetic voltage}) \\ I_M &= \frac{\omega \mu r H_r}{jZ_0} & (\text{magnetic current}) \\ V_E &= \frac{lE_\theta + \beta r E_z}{F} Z_0 & (\text{electric voltage}) \\ I_E &= \omega \epsilon_0 n^2 r E_r & (\text{electric current}). \end{aligned}$$

$Z_0 = 120\pi$  the free space impedance,  $F = ((\beta r)^2 + l^2)/r$ .

Similarly to [7], after some algebra (1) and (2) can be transformed into

$$\left. \begin{aligned} \frac{\partial V_s}{\partial r} &= \frac{-\gamma_s^2}{j\omega \epsilon_0 n F} I_s, & \frac{\partial I_s}{\partial r} &= -j\omega \epsilon_0 n F V_s \\ \frac{\partial V_d}{\partial r} &= \frac{-\gamma_d^2}{j\omega \epsilon_0 n F} I_d, & \frac{\partial I_d}{\partial r} &= -j\omega \epsilon_0 n F V_d \end{aligned} \right\} \quad (4)$$

where  $\gamma_s^2 = \beta^2 + (l/r)^2 - n^2 k_0^2 \mp (2nk_0 \beta l / ((\beta r)^2 + l^2))$  (– for  $HE_d$ , + for  $EH$  modes). Equation (4) represents two independent transmission lines with voltages  $V_s$  and  $V_d$  and currents  $I_s$  and  $I_d$ . The corresponding characteristic impedances are

$$\left. \begin{aligned} Z_s &= \frac{\gamma_s}{j\omega \epsilon_0 n F}, & Z_d &= \frac{\gamma_d}{j\omega \epsilon_0 n F}. \end{aligned} \right\} \quad (5)$$

The above equations are recognized as the well-known transmission-line equations with the solution represented by the following electric circuit (see Fig. 2) with impedances:

$$\left. \begin{aligned} Z_B &= Z_d \tanh\left(\gamma_d \frac{\delta r}{2}\right) \\ Z_P &= \frac{Z_s}{\sinh\left(\gamma_s \delta r\right)} \end{aligned} \right\} \quad (6)$$

where  $\delta r$  is the length of the transmission line.

Since  $\delta r$  is infinitesimal,  $\delta r/r \ll 1$ , we finally have

$$\left. \begin{aligned} Z_B &= \frac{1}{2}(\delta r)^2 \gamma_d^2 Z_P \\ Z_P &= \frac{Z_0}{jn r \delta r k_0 \left(\beta^2 + \left(\frac{l}{r}\right)^2\right)} \end{aligned} \right\} \quad (7)$$

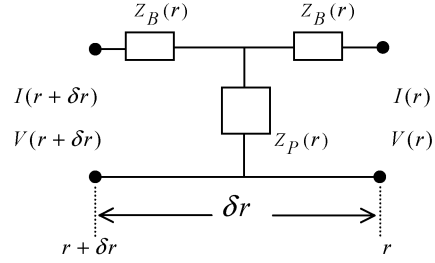


Fig. 2. Equivalent circuit of a dielectric waveguide.

Normalizing (7) with respect to  $k_0$  gives

$$\left. \begin{aligned} \bar{Z}_B &= \frac{1}{2}(\delta \bar{r})^2 \bar{\gamma}_d^2 \bar{Z}_P \\ \bar{Z}_P &= \frac{Z_0}{jn \bar{r} \delta \bar{r} \left(\bar{\beta}^2 + \left(\frac{l}{\bar{r}}\right)^2\right)} \end{aligned} \right\} \quad (8)$$

where

$$\begin{aligned} \bar{r} &= rk_0, & \delta \bar{r} &= \delta r k_0, & \bar{\beta} &= \frac{\beta}{k_0} \\ \bar{\gamma}_d^2 &= \frac{\gamma_d^2}{k_0^2} = \bar{\beta}^2 + \left(\frac{l}{\bar{r}}\right)^2 - n^2 \mp \frac{2n\bar{\beta}l}{(\bar{\beta}\bar{r})^2 + l^2} \\ \bar{Z}_P &= Z_P \times k_0, & \bar{Z}_B &= Z_B \times k_0. \end{aligned}$$

An optical fiber can be represented as a cascade of such T circuits, the impedances of which are functions of the waveguide physical and optical properties. The mode propagation constants can be determined when the optical energy is trapped inside the optical waveguide, and this is equivalent to the resonance conditions ( $Z_{total} = 0$ ) of the equivalent T circuits [6]. The normalized mode propagation constant  $\bar{\beta}$  is the function of the known fiber refractive index  $n$ , as shown in (8). We obtain the unknown  $\bar{\beta}$  using any root searching method which locates the roots of the total impedance of the T circuits,  $Z_{total} = 0$ . If the refractive index is a complex number, the calculated propagation constant should be complex. The waveguide gain or loss can therefore be derived from the imaginary part of the propagation constant.

Our approach also offers a technique for determining the  $E/M$  mode field plots of the  $HE$  and  $EH$  modes in terms of the  $I_{HE}$  and  $V_{HE}$  variables below. From the above equations, we can derive the circuit electric current  $I$  and from it the electric field  $E_r$ . From (3), we have

$$\left. \begin{aligned} V_{HE} &= \frac{V_M}{\sqrt{n(r)}} + V_E \sqrt{n(r)} \\ V_{EH} &= \frac{V_M}{\sqrt{n(r)}} - V_E \sqrt{n(r)} \end{aligned} \right\} \quad (9)$$

$$\left. \begin{aligned} I_{HE} &= I_M \sqrt{n(r)} + \frac{I_E}{\sqrt{n(r)}} \\ I_{EH} &= I_M \sqrt{n(r)} - \frac{I_E}{\sqrt{n(r)}} \end{aligned} \right\} \quad (10)$$

We can set  $I_{EH} = V_{EH} = 0$  when the  $HE$  modes are of interest. This implies that

$$\left. \begin{aligned} I_M \sqrt{n(r)} &= \frac{I_E}{n(r)} \\ \frac{V_M}{\sqrt{n(r)}} &= V_E \sqrt{n(r)} \end{aligned} \right\} \quad (11)$$

Substituting into (9) and (10), we have

$$\left. \begin{aligned} V_{HE} &= 2V_E\sqrt{n(r)}, & I_{HE} &= 2I_M\sqrt{n(r)} \\ V_{HE} &= 2\frac{V_M}{\sqrt{n(r)}}, & I_{HE} &= 2\frac{I_E}{\sqrt{n(r)}} \end{aligned} \right\}. \quad (12)$$

Note that  $V_{HE}$  and  $I_{HE}$  are also referred to as  $V_s$  and  $I_s$ , respectively, in (3). Hence

$$\left. \begin{aligned} V_E &= \frac{V_s}{2\sqrt{n(r)}}, & I_M &= \frac{I_s}{2\sqrt{n(r)}} \\ V_M &= \frac{V_s\sqrt{n(r)}}{2}, & I_E &= \frac{I_s\sqrt{n(r)}}{2} \end{aligned} \right\} \quad (13)$$

and  $I_E = \omega\varepsilon_0 n^2(r)rE_r$

Finally, we have

$$E_r = \frac{I_E}{\omega\varepsilon_0 n^2 r} = \frac{Z_0 I_E}{k_0 n^2(r)r} = \frac{Z_0 I_E}{n^2(r)\bar{r}}. \quad (14)$$

Therefore, if we already know the refractive index as a function of radius, we can use (14) to plot the electric field  $E_r$  precisely.

### III. DEFINITION OF THE COMPLEX REFRACTIVE INDEX FOR ERBIUM-DOPED FIBER

The signal gain in an EDFA is obtained by creating population inversion using a pump at 980 nm. The assumption of a three-level laser system for the EDFA provides a means of defining a complex refractive-index profile for the pumped EDFA at signal and pump wavelengths. The complex refractive-index profile of the core-doped fiber can, in general, be written as [4]

$$n(r) = \begin{cases} n_1(r) + in_i(r), & r < a \\ n_2(\text{cladding}), & r > a \end{cases} \quad (15)$$

where  $a$  is the core radius.

We illustrate our procedure by analyzing a step-index fiber with step-index erbium doping concentration in the core,  $\rho(r) = \rho_0$  for  $r < a$  and  $\rho(r) = 0$  for  $r > a$ , with  $a = 1.5 \mu\text{m}$ ,  $n_1 = 1.46$  and  $NA = 0.24$ ,  $\rho_0 = 1.6 \times 10^{25} \text{ m}^{-3}$ , and a pump wavelength of 980 nm.  $\rho(r)$  is the erbium-doping profile,  $\psi_{p,s}^2(r)$  are the fiber mode profiles at the pump and signal wavelengths, and the step-index refractive index profile are simply given by [5]

$$\psi_{p,s}^2(R < 1) = J_0^2(U_{p,s}R) \quad (16)$$

$$\psi_{p,s}^2(R > 1) = \frac{J_0^2(U_{p,s})}{K_0^2(W_{p,s})} K_0^2(W_{p,s}R) \quad (17)$$

where  $R = r/a$ ,  $U_{p,s}$ ,  $V_{p,s}$ , and  $W_{p,s}$  are the conventional fiber parameters [9] of the undoped fiber, and  $J_0(Z)$  is the Bessel function of the first kind of order zero. Equations (16) and (17) are valid only for step-index profile waveguides; for other profile waveguides, we use (14) to obtain the electric field, and the square of the field is  $\psi_{p,s}^2(r)$ .

$\sigma_a(\lambda_s)$  and  $\sigma_e(\lambda_s)$  are the absorption and emission cross sections, respectively, at signal wavelength  $\lambda_s$  and  $\eta(\lambda_s) = \sigma_e(\lambda_s)/\sigma_a(\lambda_s)$ . They correspond to of [9, Fig. 4.22], with peak values  $\sigma_{as} = 7 \times 10^{-25} \text{ m}^2$  and  $\sigma_{es} = 0.92\sigma_{as}$ . The absorption cross section of the pump is  $\sigma_{ap} = 2 \times 10^{-25} \text{ m}^2$ . Also,  $p$  and  $q$  indicate the signal and pump powers guided in the fundamental mode normalized to their respective saturation powers

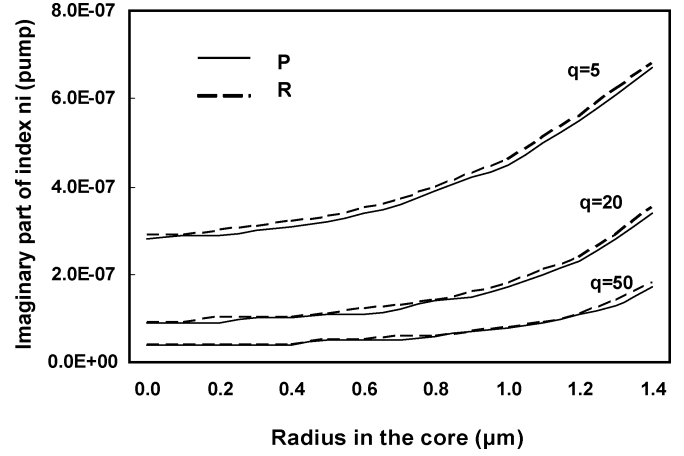


Fig. 3. Radial profile of the imaginary part of the pump index against radius in the core at different input pump power levels  $q$  (marked) by the present method (P) and Rayleigh-Ritz method (R) of [4].

$p = P_s(z)/P_{\text{sat}}(\lambda_s)$ ,  $q = P_p(z)/P_{\text{sat}}(\lambda_p)$ , with  $P_{\text{sat}}(\lambda_s)$  and  $P_{\text{sat}}(\lambda_p)$  defined as

$$P_{\text{sat}}(\lambda_s) = \frac{hc\pi\omega_s^2}{\lambda_s\sigma_a(\lambda_s)[1 + \eta(\lambda_s)\tau]} \quad (18)$$

$$P_{\text{sat}}(\lambda_p) = \frac{hc\pi\omega_p^2}{\lambda_p\sigma_a(\lambda_p)\tau} \quad (19)$$

where  $h$  is Planck's constant  $6.62 \times 10^{-34} \text{ m}^2\text{kg/s}$ ,  $c$  is the light speed in free space,  $\tau$  is the lifetime of the upper laser level  $1 \times 10^{-2} \text{ s}$ , and  $\omega_{p,s}$  is the mode power radius given by [4]

$$\omega_{p,s}^2 = 2 \int_0^\infty \psi_{p,s}^2(r)rdr. \quad (20)$$

For any medium with a complex refractive index, the imaginary part of refractive index  $n_i$  in the pumped erbium-doped fiber can be written as in [4] as follows:

$$n_i(\text{signal}) = \frac{\rho(r)\sigma_{as}\lambda_s \left[ \eta_s q |\psi_p(r)|^2 - 1 \right]}{4\pi \left[ 1 + q |\psi_p(r)|^2 + p |\psi_s(r)|^2 \right]} \quad (21)$$

$$n_i(\text{pump}) = \frac{-\rho(r)\sigma_{ap}\lambda_p \left[ 1 + \frac{\eta_s}{(1+\eta_s)p|\psi_s(r)|^2} \right]}{4\pi \left[ 1 + q |\psi_p(r)|^2 + p |\psi_s(r)|^2 \right]}. \quad (22)$$

The positive (negative) sign of the imaginary part indicates a gain (loss) medium. Once  $n_i$  is defined, the modal gain and loss can be obtained. The corresponding gain per unit length, defined as  $g = (1/p)(dp/dZ)$ , is given by  $g = 2\beta_i$ . The gain or loss of the propagation signal and pump power, in decibels per meter, is hence  $8.686k_0\beta_i$  (dB/m).

### IV. APPLICATION NUMERICAL RESULTS AND DISCUSSION

Using (15), the complex refractive-index profile, and using our transmission-line technique, we obtain the first values of complex  $n_e$  and corresponding values of gain at different wavelengths in the  $1.53\text{-}\mu\text{m}$  range. The typical radial index profiles of the imaginary part of the complex refractive index at pump and signal wavelengths, respectively, are shown in Figs. 3 and

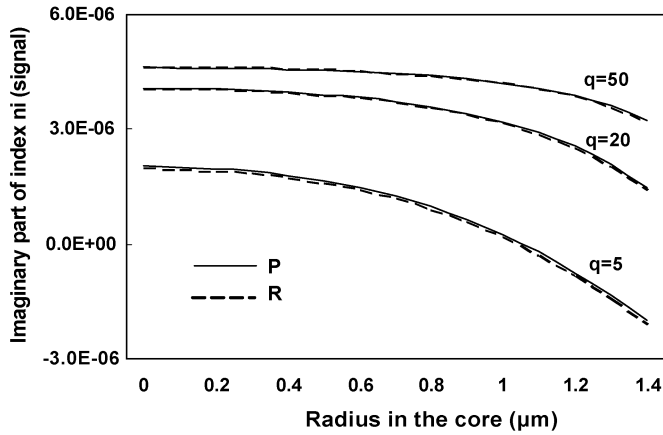


Fig. 4. Radial profile of the imaginary part of the signal index against radius in the core at different input pump power levels  $q$  (marked) by the present method (P) and Rayleigh-Ritz method (R) of [4].

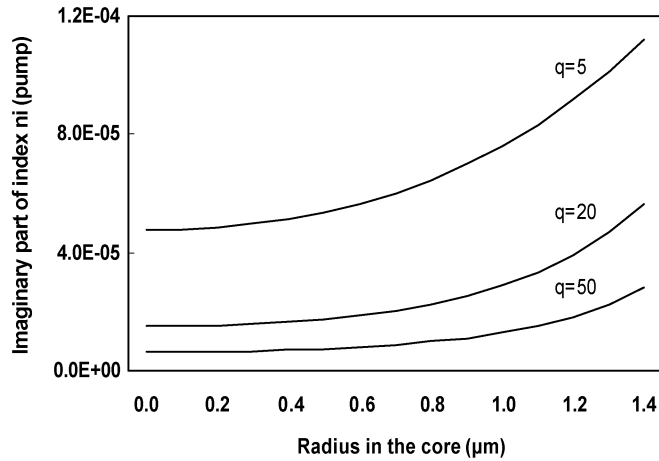


Fig. 5. Radial profile of the imaginary part of the pump index against radius in the core at various input pump power levels  $q$  (marked) by the present method (P).

4 (at  $\lambda_s = 1.53 \mu\text{m}$ ) for several pump power levels  $q$  under the small-signal approximation ( $p = 2 \times 10^{-6}$ , which corresponds to  $\sim \ln W$ ). A comparison is also shown with results in [4]. As the pump power increases, the population density in the lower level decreases, and lower steady-state absorption of pump power is obtained. Positive and negative values of  $n_i$  represent gain and loss. In Figs. 5 and 6, we show the examples for greater values for the imaginary part of the refractive index. The doping concentration in the core is now increased to  $2.68 \times 10^{27} \text{ m}^{-3}$  ( $\text{Yb}^{3+}$ ). This demonstrates that our technique is not only accurate for profiles in which the imaginary part of refractive index is very small, but can also be used for refractive index profiles with a much larger imaginary part.

A plot of signal gain for an input signal of 100 nW versus wavelength as obtained using our method and is compared to results in [5], for different values of input pump power. This is shown in Fig. 7. As expected, these results are practically coincident with the results of the more cumbersome Rayleigh-Ritz calculations. The uneven gain wavelength response of the erbium-doped fiber is also readily recognizable. It is well known that the gain flatness of an optical amplifier is very important for DWDM optical systems and that there have been many at-

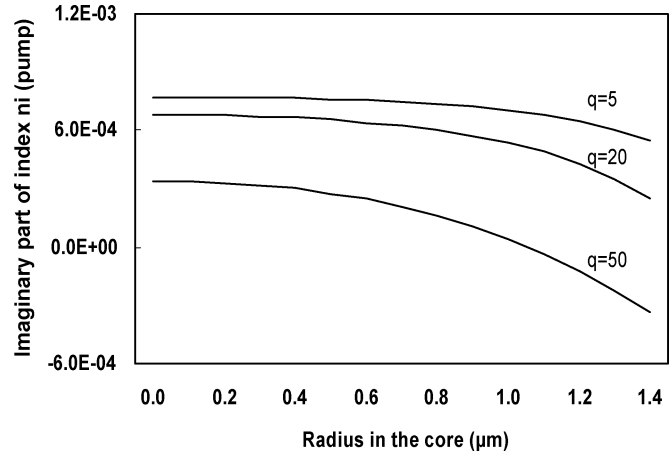


Fig. 6. Radial profile of the imaginary part of the signal index against radius in the core at various input pump power levels  $q$  (marked) by the present method (P).

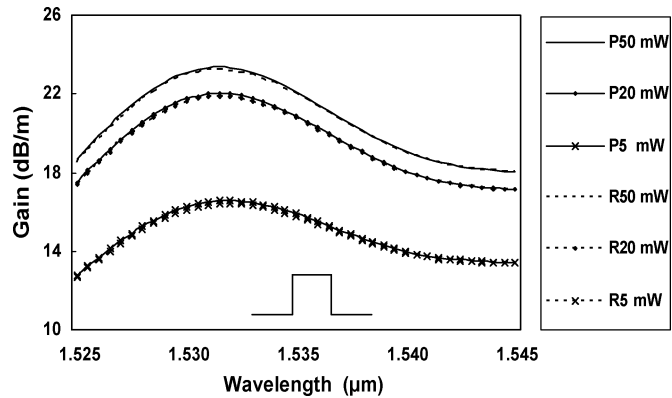


Fig. 7. Signal gain against wavelength at different input pump power levels (marked in mW) by the present method (P) and Rayleigh-Ritz method (R) of [5] (core index = 1.46, cladding index = 1.4401).

tempts to design gain-flattened optical amplifiers for this reason. Here we demonstrate that our method can be used in assisting with investigations on how to make the gain higher and flatter by modifying the optical fiber refractive index profile and the radial erbium doping concentration in the core.

#### A. Gain by Varying Refractive Index Profile

Fig. 8 shows the signal gain of a parabolic refractive index profile, but with uniform erbium doping concentration in the core. Clearly the parabolic refractive index profile step erbium-doped fiber cannot obtain the same gain as a step-index profile fiber with the same erbium doping parameters; however, the gain is flatter compared to the step index case (Fig. 7).

Fig. 9 is another example of signal gain for a doped fiber with the segmented core refractive index, but doped uniformly in the core (step). We observe that the value of the derived achieved gain is similarly not as high as that obtained from a step-index core (Fig. 7), but the overall gain curve is flatter. Fig. 10 shows the effect of gain flattening with varying the inner core index dip and for uniform core doping. We observe that the gain difference increase is insignificant with increasing inner core index. Minimum gain ripple in this case occurs when the inner core index is less than 1.4420.

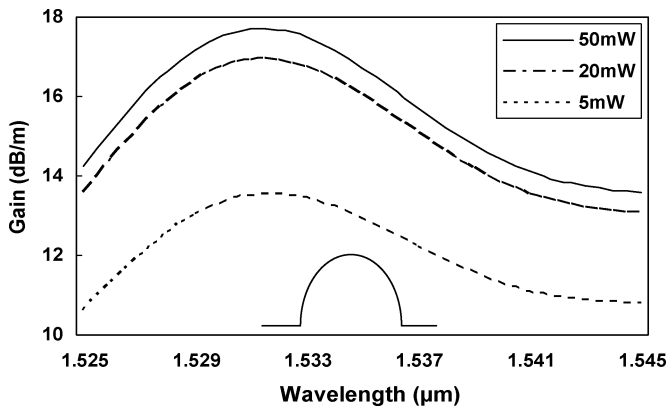


Fig. 8. Signal gain of a parabolic refractive index against wavelength at different input pump power levels (marked in mW) for parabolic index waveguide (core index = 1.46, cladding index = 1.4401).

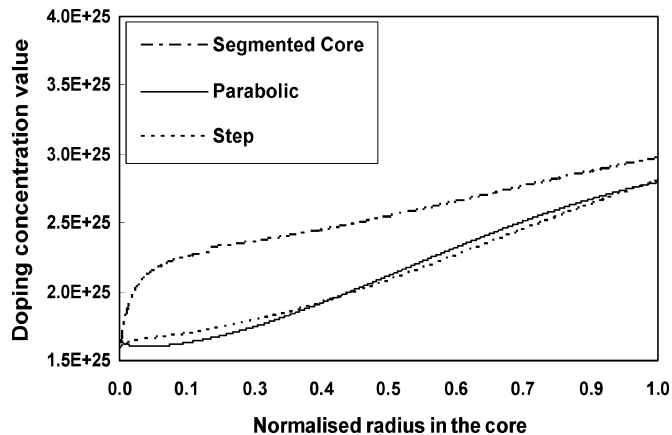


Fig. 11. Doping concentration values changing with inverse field values of different refractive index profiles fibers, used for results of Figs. 12–14.

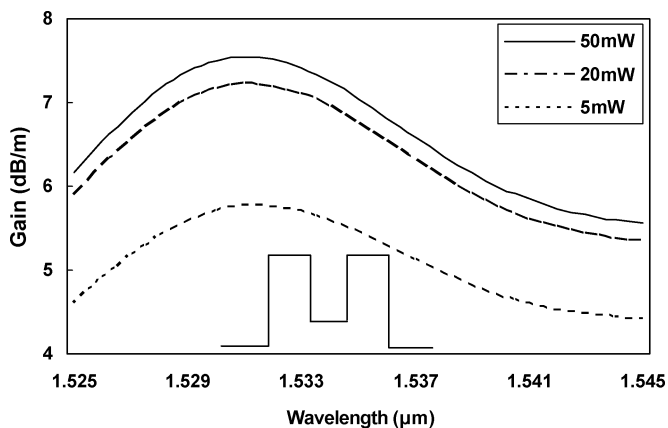


Fig. 9. Signal gain of a segmented core refractive index against wavelength at different input pump power levels (marked in mW) for the segmented core refractive index waveguide (inner core index = 1.425, core index = 1.46, cladding index = 1.4401).

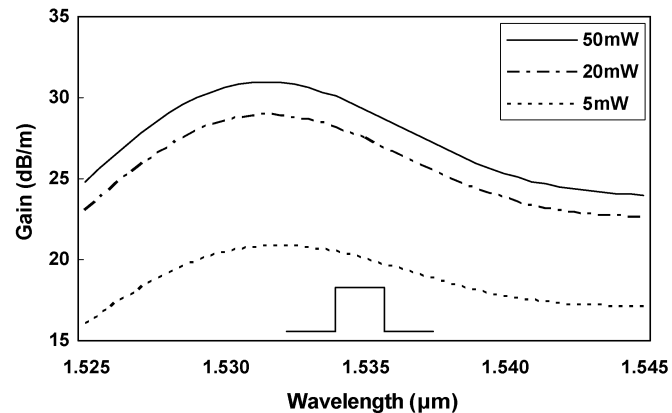


Fig. 12. Signal gain of step-index fibers against wavelength at different input pump power levels (marked in mW) using the dopant profile of Fig. 11.

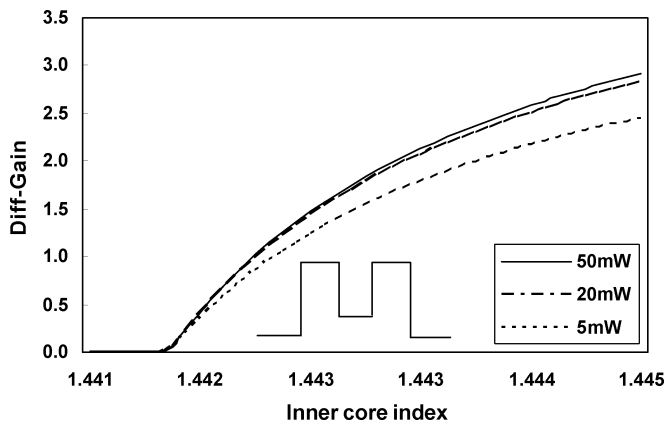


Fig. 10. Gain difference (Diff gain = Maximum gain -  $Gain_{\lambda=1.525 \mu\text{m}}$ ) against inner core index, derived from Fig. 9, at different input pump power levels (marked in mW) for the segmented core refractive index waveguide (core index = 1.46, cladding index = 1.4401).

**B. Gain by Varying Radial Doping Concentration**

The erbium amplifier gain is a function of pump power, signal wavelength, fiber length, and erbium doping concentration. Using our method, we next attempt to examine if we

have any improvements by experimenting with radially varying the (normally constant) doping concentration for different refractive index profiles. We expect this to result in an increase in the gain of the fiber amplifier. We are changing the doping concentration inversely proportional to the radial field power, multiplied by the doping constant at  $r = 0$ , of  $1.6 \times 10^{25} \text{ m}^{-3}$ . The corresponding radial doping profiles for the three different refractive index profiles considered here are shown in Fig. 11. All of the doping concentration values in the core are greater than the constant doping of  $\rho_0 = 1.6 \times 10^{25} \text{ m}^{-3}$ , but nonuniformly. Using the doping profiles of Fig. 11, we obtain the erbium amplifier gain profiles shown in Figs. 12–14. Fig. 12 shows the increased gain profile resulting for a step-index refractive index. The maximum gain is increased significantly while keeping the gain ripple nearly the same as the results in Fig. 7. Similar conclusions are drawn from Figs. 13 and 14 for parabolic and segmented core fiber index profiles, doped according to Fig. 11.

In contrast and in order to illustrate further the power of our technique, let us now consider optical fiber radial attenuation. The spectrum of optical power loss in an optical fiber is a complicated function of absorption and scattering phenomena that are introduced during the drawing of the fiber, either because of impurities introduced during the drawing or because scattering centers increase or decrease according to the level of dopant

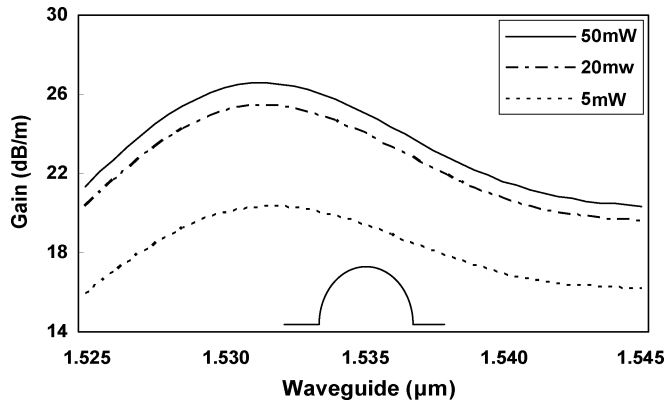


Fig. 13. Signal gain of a parabolic refractive index fibers against wavelength at different input pump power levels (marked in mW) using the dopant profile of Fig. 11.

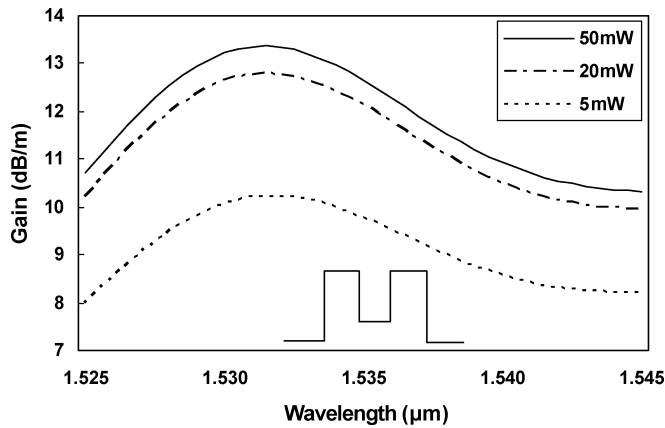


Fig. 14. Signal gain of a segmented core refractive index fibers against wavelength at different input pump power levels (marked in mW) using the dopant profile of Fig. 11.

TABLE I

$(\beta_i \times 10^{10})$  LOSS CENTERS ONLY IN THE CLADDING, STEP-INDEX FIBER  $V = 2.5$

Profiles	Exponential	Quadratic	Parabolic
Ref. 10	3.3228	3.3083	3.3059
Present Method	3.2459	3.2750	3.2662
Ratio (R10/P)	1.0236	1.0101	1.0121

used. We assume here for simplicity and for the purpose of comparison with results in [10] that only the cladding is lossy and the imaginary part of the refractive index is constant in the cladding, having the value  $5 \times 10^{-10}$ . The fiber radial attenuation results of our electric circuit resonance technique are given in Table I for a step-index single-mode fiber having  $V = 2.5$ . The table includes the results in [10] for comparison, and the agreement with our technique is demonstrated.

To allow a comparison with the recently published perturbation method [10], we assumed the following (unlikely) scenario, but one that facilitates the comparison we wish. The real part of the index is taken as a step function and we assume, therefore, that the field distribution is that of a lossless step-index fiber. However, the imaginary part of the index varies in the core according to different profiles, as shown in Fig. 15. Using our tech-

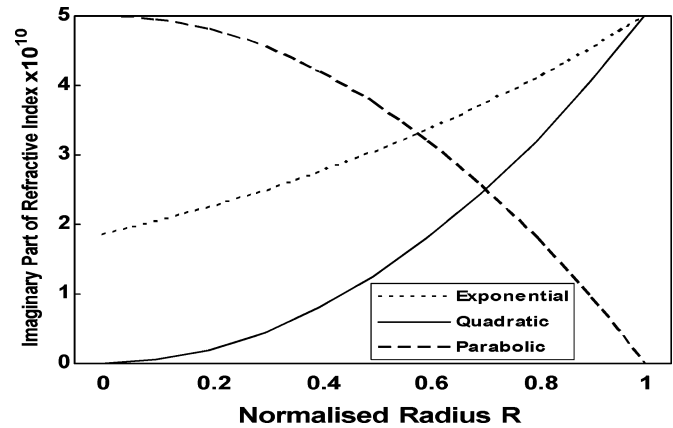


Fig. 15. Loss profiles: exponential, quadratic, and parabolic.

TABLE II

$(\beta_i \times 10^9)$  LOSS CENTERS ONLY IN THE CORE, STEP-INDEX FIBER  $V = 2.5$

Profiles	Exponential	Quadratic	Parabolic
Ref.10	1.098	0.4121	1.353
Present Method	1.0938	0.41256	1.3325
Ratio (R10/P)	1.0038	0.9988	1.0153

nique and the imaginary index profiles of Fig. 15 for the distribution of absorption or scattering centers, the attenuation is subsequently calculated. The results are given in Table II. The step-index fiber was used simply to allow comparison with published methods, but our method, as demonstrated from the tables, is accurate and can be used for determining arbitrary loss distributions and arbitrary fiber index profiles.

## V. CONCLUSION

In this paper, a new, simple, and accurate numerical procedure has been developed and demonstrated with practical examples to evaluate the exact propagation characteristics of an optical fiber with an arbitrary complex refractive-index profile. The method uses transmission-line principles and relies on the modeling of a thin uniform concentric cylindrical layer of an optical fiber to a transmission-line circuit. It may be especially useful for designing and predicting high gain (or loss) in fibers where the earlier reported approximate methods are less accurate. Finally, we have shown its practical application in amplifier design by manipulating the gain profile of typical 980-nm pumped erbium-doped fibers and also for calculating the radial attenuation of optical fibers.

## REFERENCES

- [1] S. C. Fleming and T. J. Whitley, "Measurement and analysis of pump-dependent refractive index and dispersion effects in erbium-doped fiber amplifiers," *IEEE J. Quantum Electron.*, vol. 32, pp. 1113–1121, July 1996.
- [2] J. E. Sader, "Method for analysis of complex refractive-index-profile fibers," *Opt. Lett.*, vol. 15, pp. 105–107, 1990.
- [3] A. Reisinger, "Characteristics of optical guided modes in lossy waveguides," *Appl. Opt.*, vol. 12, pp. 1015–1025, 1973.
- [4] A. Sunanda and E. K. Sharma, "Field variational analysis for modal gain in erbium-doped fiber amplifiers," *J. Opt. Soc. Amer. B*, vol. 16, pp. 1344–1347, 1999.

- [5] R. Singh and E. K. Sharma, "Propagation characteristics of single-mode optical fibers with arbitrary complex index profiles: a direct numerical approach," *IEEE J. Quantum Electron.*, vol. 37, pp. 635–640, May 2001.
- [6] C. D. Papageorgiou and A. C. Boucouvalas, "Propagation constants of cylindrical dielectric waveguides with arbitrary refractive index profile, using the 'Resonance' technique," *Electron. Lett.*, vol. 18, pp. 768–788, 1982.
- [7] A. C. Boucouvalas and C. D. Papageorgiou, "Cutoff frequencies in optical fibers of arbitrary refractive index profile using the 'Resonance' technique," *IEEE J. Quantum Electron.*, vol. QE-18, pp. 2027–2031, Dec. 1982.
- [8] A. C. Boucouvalas and X. Qian, "Optical fiber refractive index profile synthesis from near field," in *Proc. IEEE GLOBECOM*, San Francisco, CA, 2003, pp. 2669–2673.
- [9] E. Desurvire, *Erbium Doped Fiber Amplifiers*. New York: Wiley, 1994.
- [10] R. L. Gallawa, I. C. Goyal, and A. K. Ghatak, "Calculated fiber attenuation: a general method yielding stationary values," *J. Lightwave Technol.*, vol. 11, pp. 1900–1904, Dec. 1993.

**Xin Qian** (S'03) received the B.Eng degree from Tianjin University, Tianjin, China, in 2001, and he is currently working toward the Ph.D. degree at Bournemouth University, Bournemouth, U.K. His doctoral work focuses on design of optical fibers using the inverse transmission-line technique.

His research interests include fiber-based optical devices, integrated optics, and high-performance optical communication systems.

Mr. Qian is a student member of the Optical Society of America.

**Anthony C. Boucouvalas** (S'81–M'82–SM'00–F'02) received the B.Sc. degree in electrical and electronic engineering from Newcastle upon Tyne University, Newcastle, U.K., in 1978, the M.Sc. and D.I.C. degrees in communications engineering from Imperial College, University of London, London, U.K., in 1979, and the Ph.D. degree in fiber optics from Imperial College, in 1982.

Subsequently, he joined the GEC Hirst Research Center and became Group Leader and Divisional Chief Scientist working on fiber-optic components, measurements, and sensors until 1987, when he joined Hewlett Packard Laboratories (HP) as a Project Manager. At HP, he worked in the areas of optical communication systems, optical networks, and instrumentation, until 1994, when he joined Bournemouth University, Bournemouth, U.K. In 1996, he became a Professor in Multimedia Communications, and in 1999 he became Director of the Microelectronics and Multimedia research Center. His current research interests lie in optical wireless communications, optical fiber communications, multimedia communications, and human–computer interfaces. He has published over 180 papers in the areas of fiber optics, optical fiber components, optical wireless communications and internet communications, and human–computer interfaces.

Prof. Boucouvalas is a Fellow of the Institute of Electrical Engineers, a Fellow of the Royal Society for the encouragement of Arts, Manufacturers and Commerce, (FRSA), and a Member of the New York Academy of Sciences, and ACM. He is an Editor of the IEEE WIRELESS COMMUNICATIONS MAGAZINE, IEEE TRANSACTIONS ON WIRELESS NETWORKS, and *EURASIP Journal on Wireless Communications and Networks*, and he is Secretary of the IEEE UK&RI Communications Chapter. He is a member of the Organizing Committee of the International Symposium on Communication Systems Networks and Digital Signal Processing, (CSNDSP), Vice Chair of IEEE GLOBECOM 2003 for Optical Networking and Systems, and a member of Technical Committees in numerous conferences.